



# Investigating the Performance of Solar Steam Generation Using a Carbonized Cotton-Based Evaporator

Haoming Chen<sup>1</sup>, Yuchao Chen<sup>2</sup>, Jinqi Zang<sup>2</sup>, Changchang Sha<sup>2</sup>, Yupeng Xiao<sup>2</sup>, Wenju Wang<sup>2\*</sup>, Haihou Wang<sup>3\*</sup> and Juai Wu<sup>4\*</sup>

<sup>1</sup>School of Environmental and Biological Engineering, Nanjing University of Science and Technology, Nanjing, China, <sup>2</sup>School of Energy and Power Engineering, Nanjing University of Science and Technology, Nanjing, China, <sup>3</sup>Taihu Research Institute of Agricultural Sciences, Suzhou, China, <sup>4</sup>College of Automation and College of Artificial Intelligence, Nanjing University of Posts and Telecommunications, Nanjing, China

## OPEN ACCESS

### Edited by:

Hsien-Yi (Sam) Hsu, City University of Hong Kong, Hong Kong SAR, China

### Reviewed by:

Muhammad Amjad, University of Engineering and Technology, Pakistan  
Haochun Zhang, Harbin Institute of Technology, China

### \*Correspondence:

Wenju Wang  
wangwenju@njupt.edu.cn  
Haihou Wang  
wanghaihou@126.com  
Juai Wu  
wujuai@njupt.edu.cn

### Specialty section:

This article was submitted to Solar Energy, a section of the journal Frontiers in Energy Research

**Received:** 18 November 2021

**Accepted:** 07 March 2022

**Published:** 09 May 2022

### Citation:

Chen H, Chen Y, Zang J, Sha C, Xiao Y, Wang W, Wang H and Wu J (2022) Investigating the Performance of Solar Steam Generation Using a Carbonized Cotton-Based Evaporator. *Front. Energy Res.* 10:817638. doi: 10.3389/fenrg.2022.817638

Solar-driven steam generation as a potential green technology has attracted extensive attention to solve the freshwater scarcity crisis. Photothermal materials as the key section of solar steam generation have been widely reported. However, there is still a challenge in developing easily prepared, environmental-friendly, and low-cost materials. Herein, the simple, scalable, and porous carbonized cotton was prepared as an evaporator to enhance solar-based evaporation, which has excellent light absorption ability in the range of the full spectrum (300–2,500 nm). Benefiting from 95% solar absorption and the pores between the cellulose tubes, the carbonized cotton heated by plate carbonization reaches a steam generation rate of  $0.8 \text{ kg m}^{-2} \text{ h}^{-1}$ , which is about 5 times that of untreated cotton. Compared with tube furnace carbonization, flat plate heating carbonization of cotton requires lower equipment requirements and does not need nitrogen protection and cleaning tar, and the photothermal conversion efficiencies of both are similar. In addition, carbonized cotton as an evaporator was heated up rapidly under 1 sun irradiation and reached a stable temperature in 20 s, greatly improving the photothermal conversion rate. Therefore, plate heating carbonized cotton provides a good idea for preparing solar photothermal conversion materials and a novel strategy for simplifying the production of biomass thermal evaporators.

**Keywords:** cotton, biomass carbon material, photothermal conversion, solar steam generation, clean water production

## INTRODUCTION

Water is the basic element of life, economic development, and social progress. However, with the rapid growth of the global population, the supply of clean water resources will become tense in the following decades (Bartram et al., 2014; Xu et al., 2020; Xu et al., 2021a). Although the traditional thermal distillation technology can alleviate the problem of water shortage (Ortiz et al., 2005; Wang et al., 2019a; Xu et al., 2021b), it consumes a lot of coal and other fossil fuels and causes a lot of energy waste and further pollution problems (Wang et al., 2019b; Xue et al., 2019). Solar energy is one of the largest available renewable resources. Using solar energy to drive water evaporation to produce clean water is an effective way to solve the problem of water shortage (Kuravi et al., 2013; Alvarez et al., 2018; Nathan et al., 2018; Jun et al., 2019). However, the low absorption rate of water to solar energy hinders its practical application.

Therefore, it is necessary to apply materials with a wide solar absorption spectrum and a high conversion efficiency to break through this bottleneck (Xu et al., 2021c). At present, the absorption materials used for solar thermal conversion mainly include the following categories: precious metal materials (Wang et al., 2014; Chang et al., 2016), semiconductor materials (Bao et al., 2016; Song et al., 2018; Wu et al., 2019a), organic molecular materials (Liu et al., 2013), and carbon-based materials (Liu et al., 2015; Li et al., 2016; Li et al., 2017; Wu et al., 2019b). Carbon-based materials have development prospects and application potential due to their low cost, richness content, excellent light absorption capacity, and high efficiency for light-to-heat conversion.

However, some carbon materials, such as graphene oxide, with complex preparation processes and relatively high costs are applied less in industries. Therefore, biomass materials with a wide range of sources, low cost, and natural hydrophilicity have attracted the attention of researchers. Cellulose ( $C_6H_{10}O_5$ ) is a polysaccharide composed of macromolecules and is ubiquitous in natural organisms. The carbon content of cellulose is extremely high (more than 50%). There are a large number of hydroxyl groups in the molecular chain of cellulose, so cellulose possesses superior hydrophilic properties. In addition, the hydrogen bonds in cellulose make cellulose stable and will not break at room temperature. Cellulose is a low-cost renewable material that has been widely produced and applied. Moreover, cotton, with over 90% cellulose content, is one of the most important sources of natural cellulose. At present, cotton is mainly used for making textiles and is also used in the beauty industry. As a biomass with a low impurity content, cotton is one of the ideal raw materials to prepare biomass carbon.

Biomass carbon materials are generally formed by high-temperature pyrolysis in an inert gas atmosphere. For example, Chen Y. et al. (2020) carbonized the sunflower heads that have a naturally 3D macrostructure at a high temperature to obtain a 3D-structured photothermal conversion device. The light-to-heat conversion efficiency under 1 sun of light was more than 90%. Fang et al. (2018) used the natural 3D structure of the showerhead to prepare a lotus-shaped bionic evaporator by high-temperature pyrolysis. The evaporator has good wettability and a hydrophobic surface. The evaporation efficiency is up to 90% under 1 sun of light. The main problems of biomass-based photothermal conversion devices are a relatively insufficient water evaporation rate (WER), a low heat conversion efficiency, and a complicated synthesis process. Considering that the real biomass faces problems such as peeling pretreatment and fruit transportation and storage, it must be freeze-dried, which prolongs the production cycle of photothermal materials and increases power consumption. However, conventional biomass carbonization methods, such as high-temperature pyrolysis carbonization or hydrothermal carbonization, cause relatively high power consumption and are accompanied by by-products, and equipment cleaning is time-consuming and labor-intensive.

In order to prepare carbon materials with application prospects and economic benefits, in this work, we conduct flat heating carbonization on cotton, which takes a much shorter time than conventional methods, and barely any by-products are produced during the carbonization process. At the same time, cotton was carbonized in a tubular furnace at the same carbonization temperature. When comparing these two methods, we found that the flat heating carbonization method with the same carbonization temperature can greatly simplify the preparation process without reducing the steam generation rate. The carbonized cotton was ground to powder and deposited on untreated cotton by the solution deposition method for comparison. In addition, this work further designs a double-layer floating system using the prepared biomass carbon material (Chen et al., 2017; Liu et al., 2017). The system consists of a light-to-heat conversion part and an external water transport part. The cotton column on the cold evaporating surface is introduced as a water transport device to reduce the heat loss of the solar-based evaporation system.

## EXPERIMENTAL

### Materials Preparation

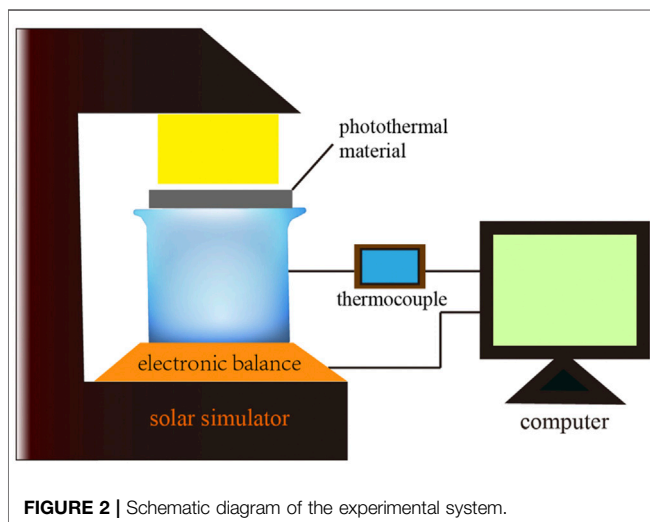
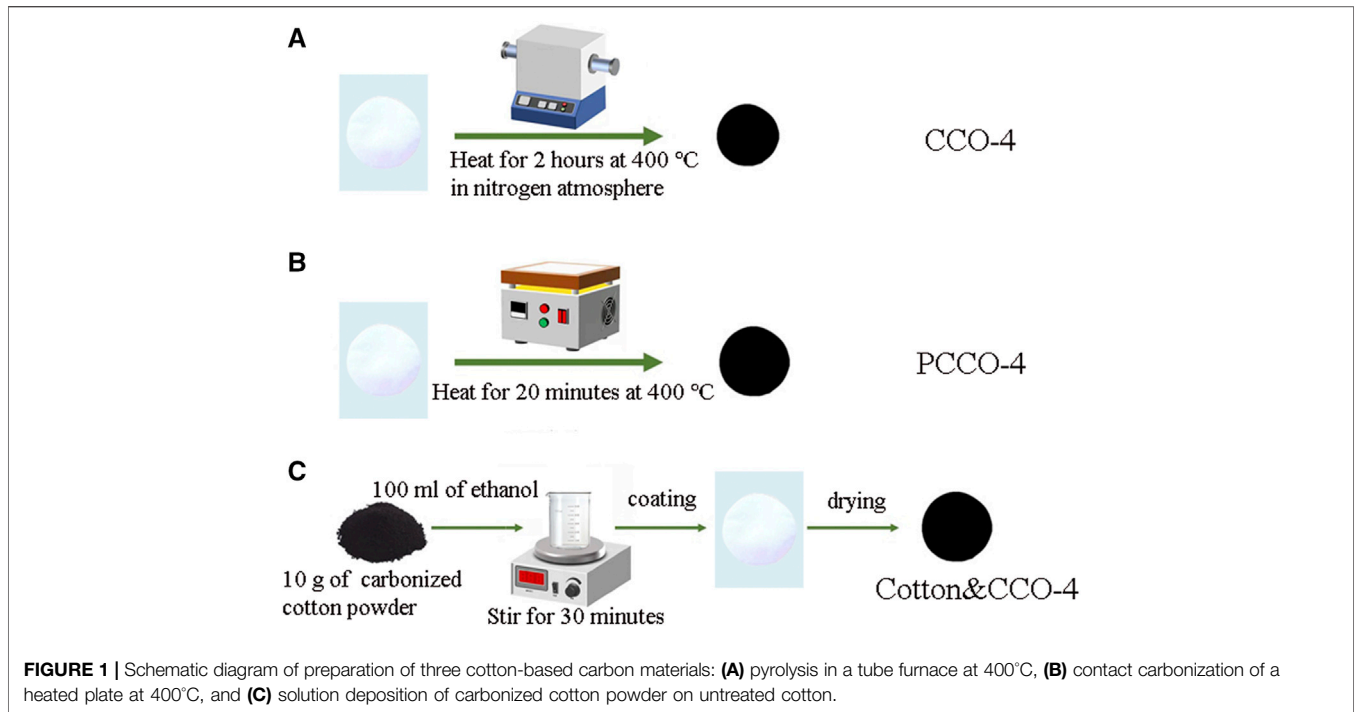
The cotton pad was ultrasonicated two times with ethanol for 30 min. After drying, the cotton pad was heated on a heating plate at 400°C for 20 min to carbonize one side and marked as CCO-4. On the other hand, the same size of the cotton pad after ultrasound and drying was heated to 400°C at a heating rate of 5°C/min in a nitrogen-filled tube furnace for 2 h. After cooling, the sample was marked as PCCO-4. Finally, the grated carbonized cotton powder (PCCO-4) was deposited on the untreated side of the same cotton pad by solution deposition, marked as Cotton & CCO-4, as shown in **Figure 1**.

### Design of 2D Water Channels

Cotton with good water delivery ability is used as the bottom layer to form a double-layer structure of the solar evaporation system. The ultrasound-cleaned cotton was paved and cut into rectangles of 6 × 20 cm, then rolled to a height of 0 cm (minus container height). The cotton column was put into the beaker until the beaker was fully filled, and water was slowly injected so that the cotton column was completely infiltrated. Finally, carbonized cotton was placed on the top of the cotton column to form a double-layer solar energy evaporation system. The moisture transfer and water evaporation on the material surface formed a dynamic balance, as shown in **Figure 2**. The experimental platform mainly includes three parts, which are the light source system, steam generation system, and measurement and acquisition system. The light source system uses a model SS150A artificial simulated solar emitter to provide stable light energy for steam generation.

### Characterization

Scanning electron microscopy (SEM, EM30, COXEM, Korea) was used to characterize the microscopic morphology and structure of carbonized cotton under an accelerating voltage



of 10 kV. With KBr as the background material, the functional group of the material was tested with a Fourier transform infrared (FTIR) spectrometer of the Shidazu model IRA-15WL. The X-ray diffraction pattern was measured using a Bruker AXS D8 Advance X-ray diffractometer. The test range was  $2\theta$  from  $10^\circ$  to  $80^\circ$ , the scanning rate was  $2^\circ/\text{min}$ , the voltage was 40 kV, and the current was 50 mA. An Agilent CARY 5000 ultraviolet–visible–near-infrared spectrophotometer was used to measure the light absorption efficiency of the material in the range of 200–2,500 nm. The surface temperature of the material is measured with a thermal imager (FLIR C5).

## Theoretical Background

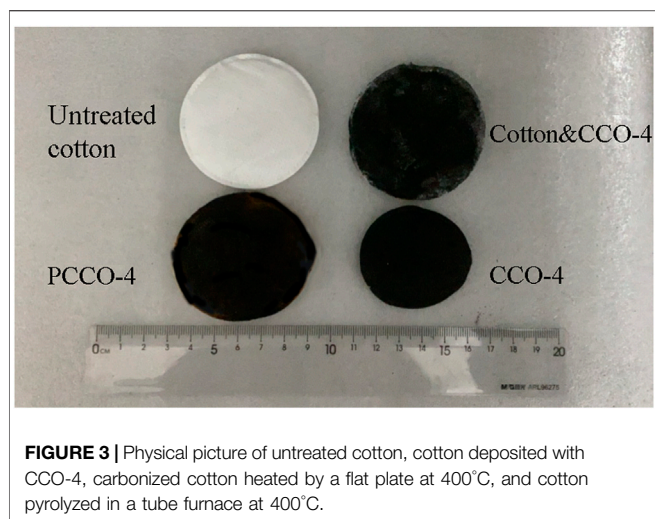
Consider that the solar heat conversion efficiency can directly evaluate the performance of solar steam generation. The solar energy is eventually converted into heat, which leads to useful water evaporation and heat loss (e.g., thermal radiation, convection, and conduction). According to the WER evaluation that fundamentally determines the performance of the solar-based evaporation, the solar heat conversion efficiency ( $\eta$ ) is defined as (Amjad et al., 2017; Amjad et al., 2018; Wu et al., 2019b; Khalil et al., 2020):

$$\eta = \frac{m(h_{LV} + Q)}{C_{opt}q_i} \quad (1)$$

$$h_{LV} = 1.91846 \times 10^3 \left[ \frac{T_i}{T_i - 33.91} \right]^2 \text{ J/g} \quad (2)$$

where  $\eta$  represents the solar light-steam conversion efficiency,  $m$  is the net mass change after deducting the dark evaporation ( $\text{kg m}^{-2}\text{h}^{-1}$ ),  $h_{LV}$  is the latent heat enthalpy ( $\text{J kg}^{-1}$ ), and  $Q$  is the sensible heat for increasing the water temperature.

$Q = c(T_i - T_0) \text{ J kg}^{-1}$ ,  $c = 4.2 \text{ J g}^{-1}\text{K}^{-1}$ ,  $T_0$  is the initial temperature of water,  $T_i$  is the temperature of evaporation at the gas/liquid interface (K),  $q_i$  is the solar radiation value of a sun, and  $C_{opt}q_i$  is the total power density of the sun. There are several factors that affect the calculation of solar thermal conversion efficiency: temperature, humidity, airflow, and evaporation area in the laboratory test environment. It is worth noting that  $m$  is the net WER after subtracting the WER in the dark environment; thus, the influence of the environment on the experiment can be eliminated. Latent heat is the enthalpy of phase change, which varies from 2,453 to 2,265  $\text{kJ kg}^{-1}$  from 20 to 100°C.



## RESULTS AND DISCUSSION

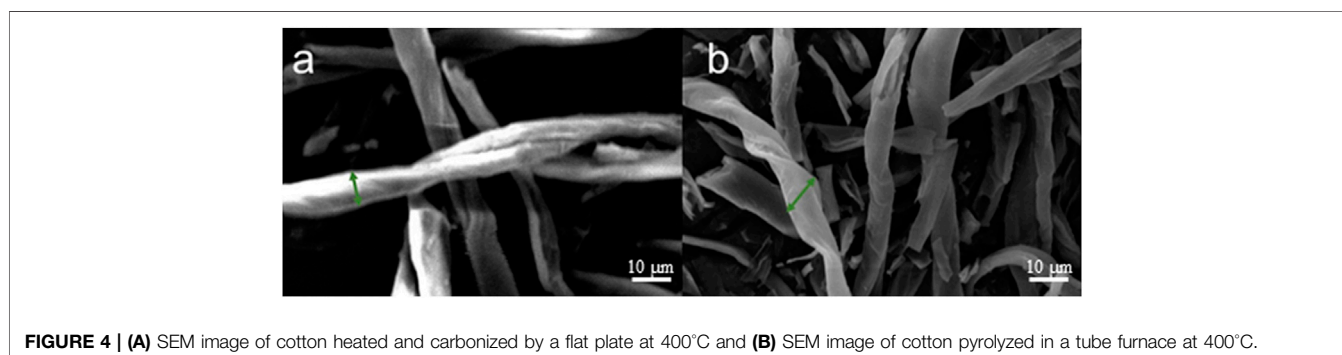
The optical photographs of cotton-based carbon materials prepared by different carbonization methods and untreated cotton are shown in **Figure 3**. It can be seen clearly that the size of cotton which has been carbonized by flat heating on one side is slightly smaller than that of untreated cotton, but the difference is not significant. Because the heating and carbonization of the plate happened directly on one side and in close contact, some less material is decomposed during the carbonization process. In contrast, the size of the pyrolyzed cotton in the tube furnace is significantly reduced because the cotton completely placed in the tube furnace is carbonized more thoroughly, and more structures are destroyed and decomposed. The size of the cotton deposited with CCO-4 does not change, and CCO-4 overcomes the problem of poor light absorption of cotton. Therefore, the composite material has the potential as a light-to-heat conversion device.

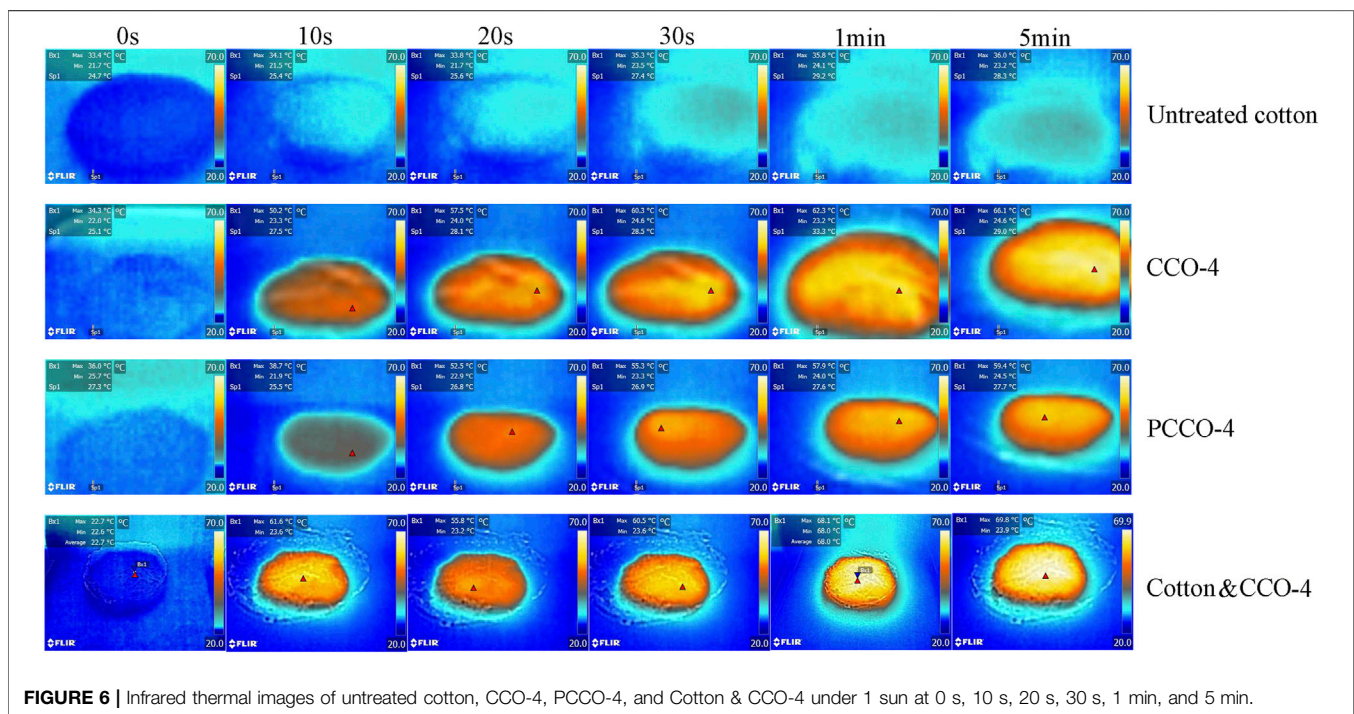
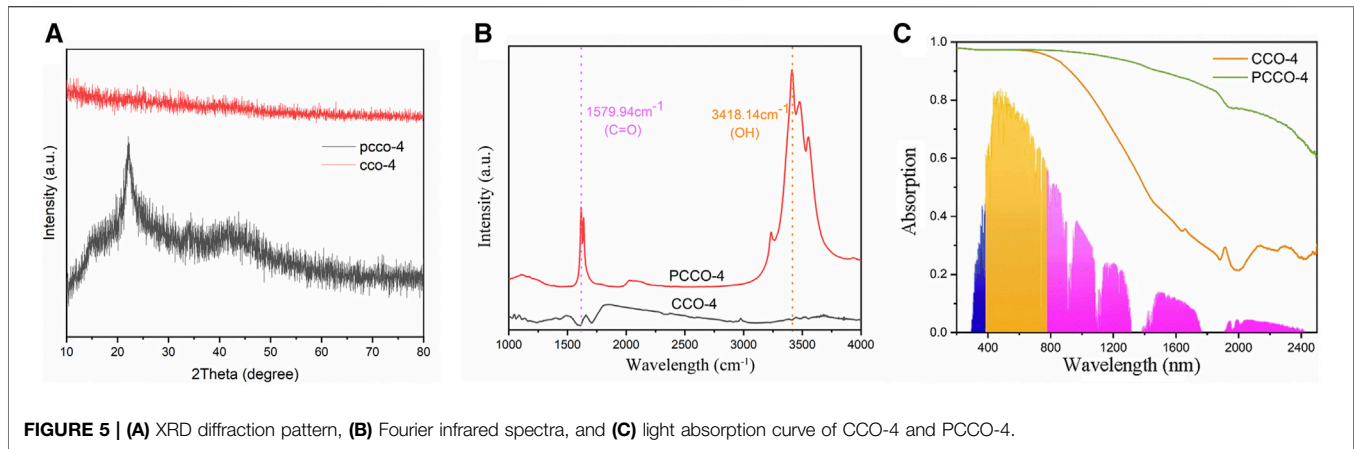
The SEM images of carbonized cotton heated by a flat plate at 400°C and cotton pyrolyzed in a tube furnace (shown in **Figure 4**) indicate that the high temperature destroys the continuity of the original fiber structure and makes it more irregular. This microstructure is conducive to better capture of photons, so it has a high broad-band absorption capacity and improves the light

absorption efficiency (Wu et al., 2019c; Chen L et al., 2020). The pores between the fiber tubes are a good way to increase the space for water transport. In contrast, the pyrolyzed cotton of the tube furnace has more damaged structures, so the fiber pipes are stacked together, thus presenting a denser image.

The oxygen and hydrogen of the pyrolyzed and carbonized cotton escaped in the form of gaseous water after carbonization, and the carbonized cotton was characterized by XRD, as shown in **Figure 5A**. The XRD diffraction pattern of PCCO-4 has a diffuse diffraction peak between 23° and 26°. This is the main feature of amorphous carbon, indicating that the material contains amorphous carbon. Amorphous carbon can improve the efficiency of light transfer (Wilson et al., 2020). However, CCO-4 has no obvious peaks, indicating that its amorphous carbon structure is relatively inconspicuous. Functional groups of carbonized cotton were identified by Fourier transform infrared spectroscopy (FTIR) analysis, as shown in **Figure 5B**. The peaks in the FTIR spectra for PCCO-4 are observed at 1,579.94 and 3,418.14  $\text{cm}^{-1}$ , responding to C=O and OH, respectively. It can prove the excellent hydrophilicity of the material (Yang et al., 2017). In contrast, CCO-4 does not have any prominent peaks, and only a weaker peak appears near 1,579.94  $\text{cm}^{-1}$ , indicating that its hydrophilicity is far inferior to that of PCCO-4.

To quantitatively characterize the photoabsorption ability of the carbonized cotton, we recorded absorption spectra in the solar spectral range (wavelengths from 200 to 2,500 nm), as shown in **Figure 5C**. The light absorption of PCCO-4 is 95%, which is higher than that of CCO-4 (84%). Among them, there is no difference between the two samples in the ultraviolet range, and their light absorption efficiencies are both very high. However, PCCO-4 shows a higher light absorption rate than CCO-4 in the visible wavelength range close to infrared, especially in the infrared range as shown in **Table 1**. However, for the photothermal conversion of amorphous biochar, the longer-wavelength light in the infrared range can hardly reach the threshold of photothermal conversion and cannot be used by the material. Furthermore, visible light and infrared account for 99% of the total radiant energy, and near-infrared occupies about 90% of the energy in infrared. Therefore, the solar energy absorption rate of the photothermal conversion device depends on the absorption of visible light and near-infrared (Ghasemi et al., 2014). CCO-4 and PCCO-4 have little





difference in light absorption in the visible and near-infrared regions, so the total light absorptions of the two samples are similar. Because light-to-heat conversion has certain requirements for the energy of photons, the difference between the two samples in the solar-based evaporation will be further reduced.

The temperature distribution and the average temperature of the carbonized cotton surface were estimated using a thermal camera under 1 sun illumination, as shown in **Figure 6**. The room temperature was between 21 and 27°C, and the humidity was about 35%. It can be seen clearly from the figure that the photothermal performance of untreated cotton is poor. Almost all carbonized cottons show a significant temperature rise within only half a minute, while the infrared image of

untreated cotton does not show any obvious heating phenomenon. The surface temperature of CCO-4, PCCO-4, and Cotton & CCO-4 reaches 55.4, 57.4, and 65.2°C after 5 min under the light intensity of 1 kW m<sup>-2</sup>, respectively. This is because the light absorption performance of untreated cotton is poor, and the conversion efficiency of light and heat performance is low. Among them, the difference in the photothermal conversion performance of CCO-4 and PCCO-4 is very small, indicating that the different carbonization methods of cotton have no significant impact on the photothermal conversion capacity. While the photothermal conversion capacity of Cotton & CCO-4 is significantly better than those of the other two carbon materials, because of the excellent light absorption and light-to-heat conversion

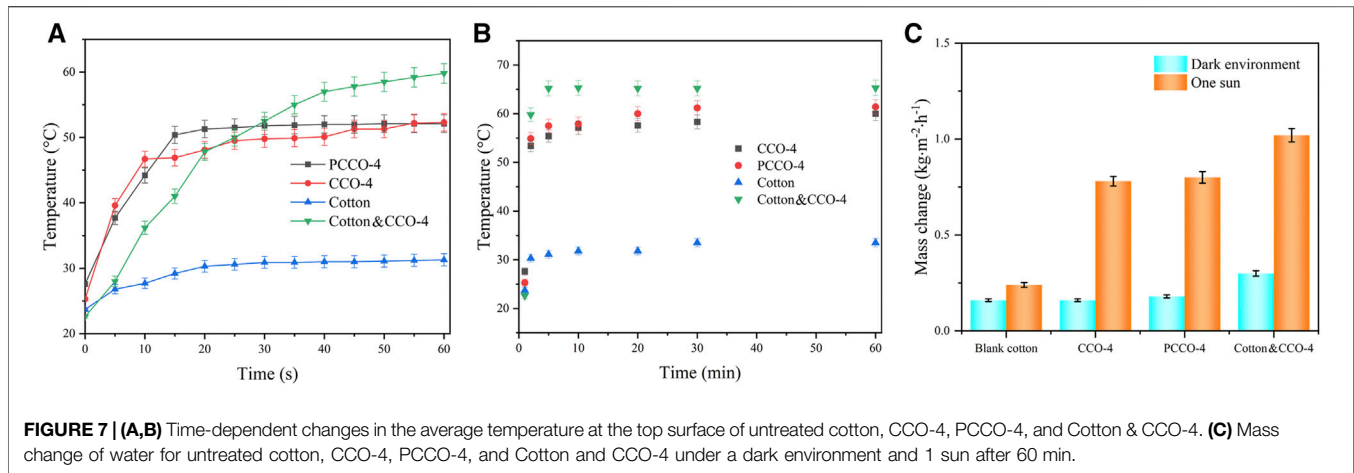


**TABLE 1 |** Light absorption efficiency of carbonized cotton prepared under different pyrolysis conditions.

Samples	Visible light area (%)	Invisible light band (%)	Full solar spectrum (%)
CCO-4	97	51	84
PCCO-4	97	86	95

capabilities of the carbonized cotton, the loading of powdered carbon particles on the cotton increases its surface roughness, making it more perfect in capturing photons.

The Profession FLIR Tool and software were used to collect the temperature data and the average temperature on the surface of the material. The resulting temperature–time image is shown in **Figure 7**. **Figure 7A** shows the average temperature of the material surface within 0–60 s, and the data collection interval is 5 s. **Figure 7B** shows the average temperature of the material surface within 0–60 min. The data from 0 to 5 min are consistent with **Figure 7A**, and the subsequent data collection times are 10, 20, 30, and 60 min. It can be seen from **Figure 7A** that the surface temperature of the untreated cotton is kept at about  $31 \pm 0.8^\circ\text{C}$  from 0 to 30 s. Even after 1 h, it only reaches  $33.5 \pm 0.9^\circ\text{C}$ . In contrast, the light-to-heat conversion rate of PCCO-4 and CCO-4 is faster. Their surface temperatures stabilize in 20s and eventually reach  $61.4 \pm 1.5^\circ\text{C}$  and  $60 \pm 1.4^\circ\text{C}$  in about an hour, showing similar photothermal conversion properties. However, the surface temperature of Cotton & CCO-4 still showed a trend of rapid increase after 1 min of 1 sun illumination, stabilized at  $65.2 \pm 1.6^\circ\text{C}$  in about 5 min, and finally reached  $65.3 \pm 1.6^\circ\text{C}$  in about 1 h. Therefore, both CCO-4 and PCCO-4 showed a rapid temperature rise in 20 s

and a slow temperature rise in the following 0.5 h. The temperature rise of Cotton & CCO-4 mainly occurred within the first 5 min.

There is an upper limit to the improvement of the photothermal efficiency of biomass-based carbon photothermal conversion devices. The current main solar-based evaporation system using biomass carbon materials as the photothermal conversion device is generally a floating system, which has a relatively high heat loss. Therefore, a double-layer floating system was further designed for the prepared biomass carbon material, which was composed of a photothermal conversion device and an external water transport device. In this paper, a cotton column with a cold evaporating surface was introduced as a water transport device. Solar-based evaporation experiments were carried out using the above-mentioned biomass carbon materials. The experiments were carried out on the above biomass carbon materials under environmental conditions of  $19\text{--}22^\circ\text{C}$  and about 40% humidity. The beaker was filled with a cotton column equal to the height of the beaker as a water transport channel, and it was filled with water to completely soak. As a water transport channel, pure cotton and carbonized cotton that are completely infiltrated by water can be closely connected with each other to complete water transport. Carbonized cotton relies on the capillary effect of its own pores to transport water to the top surface, where the water at the interface is heated and evaporates due to the high temperature of the top surface of photothermal materials.

The evaporation rate of photothermal water is shown in **Figure 7C**. Under dark evaporation conditions, the water evaporation rates of CCO-4 and the pure cotton column are close to the same. In addition, the dark evaporation rate of PCCO-4 is  $0.18 \pm 0.01 \text{ kg m}^{-2} \text{ h}^{-1}$ , slightly higher than the

**TABLE 2 |** Solar-to-steam conversion efficiency of cotton biochar.

Sample	Net steam generation rate	Light-steam conversion efficiency (%)
CCO-4	$0.62 \text{ kg m}^{-2} \text{ h}^{-1}$	42
PCCO-4	$0.62 \text{ kg m}^{-2} \text{ h}^{-1}$	42
Cotton & CCO-4	$0.72 \text{ kg m}^{-2} \text{ h}^{-1}$	49

$0.16 \pm 0.01 \text{ kg m}^{-2} \text{ h}^{-1}$  of the other two, while Cotton & CCO-4 exhibits a higher  $0.3 \pm 0.02 \text{ kg m}^{-2} \text{ h}^{-1}$  due to its pores and large evaporation area of the carbonized cotton. Under 1 sun of light, the cotton column without the photothermal material only showed  $0.24 \pm 0.01 \text{ kg m}^{-2} \text{ h}^{-1}$  because the light absorption efficiency of untreated cotton is low and the photothermal performance is poor. CCO-4 and PCCO-4 still show similar evaporation rates of  $0.78 \pm 0.04$  and  $0.8 \pm 0.04 \text{ kg m}^{-2} \text{ h}^{-1}$ , respectively. On the other hand, Cotton & CCO-4 shows superior solar based evaporation performance, and its water evaporation rate is  $1.02 \pm 0.05 \text{ kg m}^{-2} \text{ h}^{-1}$ .

The light-steam conversion efficiency of cotton biochar prepared by different carbonization methods is calculated, and the results are shown in **Table 2**. It can be seen that the net steam generation rates of cotton carbons with the same carbonization temperature by different carbonization methods (plate contact heating carbonization and tube furnace carbonization) are the same, although SEM, XRD, FTIR, ultraviolet-visible-infrared spectroscopy, and the light absorption test of CCO-4 and PCCO-4 show obvious differences. The results of the thermal heating test of them are similar, which means that although the carbonization method has changed the thermophysical properties of cotton biochar to a certain extent, it has almost no effect on the photothermal performance. However, the size change of the cotton carbonized by flat contact carbonization is smaller than that of the cotton heated and carbonized by the tube furnace, and it is more convenient and feasible. Therefore, if it is expanded to industrial production, flat contact carbonization will have a greater application prospect.

## CONCLUSION

In summary, we have designed a novel, highly efficient photothermal conversion material for solar steam generation using carbonized cotton, one of the low-cost agricultural products. As a cellulose material, cotton has outstanding solar absorption and excellent hydrophilicity. The steam generation rates of carbonized cotton heated by plate carbonization and tube furnace carbonization are 0.8 and  $0.78 \text{ kg m}^{-2} \text{ h}^{-1}$  under 1 sun, which are about 5 times that of untreated cotton. However, the plate heating carbonization method requires simpler equipment and lower sample specifications, does not require nitrogen protection, does not produce a large amount of harmful substances such as tar, and consumes lower electricity costs. Therefore, plate heating carbonized cotton provides a good idea for preparing solar photothermal conversion materials on

## REFERENCES

- Alvarez, P. J. J., Chan, C. K., Elimelech, M., Halas, N. J., and Villagrán, D. (2018). Emerging Opportunities for Nanotechnology to Enhance Water Security. *Nat. Nanotech* 13 (8), 634–641. doi:10.1038/s41565-018-0203-2
- Amjad, M., Jin, H., Du, X., and Wen, D. (2018). Experimental Photothermal Performance of Nanofluids under Concentrated Solar Flux. *Solar Energ. Mater. Solar Cell* 182, 255–262. doi:10.1016/j.solmat.2018.03.044
- Amjad, M., Raza, G., Xin, Y., Pervaiz, S., Xu, J., Du, X., et al. (2017). Volumetric Solar Heating and Steam Generation via Gold Nanofluids. *Appl. Energ.* 206, 393–400. doi:10.1016/j.apenergy.2017.08.144
- Bao, T., Yin, W., Zheng, X., Zhang, X., Yu, J., Dong, X., et al. (2016). One-pot Synthesis of PEGylated Plasmonic MoO<sub>3</sub>-X Hollow Nanospheres for Photoacoustic Imaging Guided Chemo-Photothermal Combinational

a larger scale and at a lower cost. It is worth noting that cotton and CCO-4, as a photothermal conversion material with CCO-4 deposited on the surface of cotton, can generate steam at a rate of  $1.02 \text{ kg m}^{-2} \text{ h}^{-1}$  under 1 sun. Due to the extremely strong adsorption of cotton to the particles, the carbon particles are only adsorbed on the surface of the cotton to increase the absorption of light and strengthen the photothermal effect. Therefore, the carbonized cotton is promising to be applied in real solar steam generation equipment.

## DATA AVAILABILITY STATEMENT

The original contributions presented in the study are included in the article/**Supplementary Material**, further inquiries can be directed to the corresponding authors.

## AUTHOR CONTRIBUTIONS

WW, HW, and JW conceived the presented idea. HC and YC carried out the experiment. CS wrote the manuscript with support from all authors. JZ and YX revised the manuscript. All authors provided critical feedback and helped shape the research, analysis, and manuscript.

## FUNDING

This work was financially supported by the National Natural Science Foundation of China, China (No. 21676148), and the Fundamental Research Funds for the Central Universities, China (No. 30918012202). X-ray diffraction was performed at the Materials Characterization Facility of Nanjing University of Science and Technology. This work was also supported by the National Natural Science Foundation of China project (No. 42007105), the Natural Science Foundation of Jiangsu Province (BK20181165), and the 5th Scientific Research Project of the “333 High-level Talents Training Project” of Jiangsu Province (BRA2020128).

## SUPPLEMENTARY MATERIAL

The Supplementary Material for this article can be found online at: <https://www.frontiersin.org/articles/10.3389/fenrg.2022.817638/full#supplementary-material>

- Therapy of Cancer. *Biomaterials* 76, 11–24. doi:10.1016/j.biomaterials.2015.10.048
- Bartram, J., Brocklehurst, C., Fisher, M., Luyendijk, R., Hossain, R., Wardlaw, T., et al. (2014). Global Monitoring of Water Supply and Sanitation: History, Methods and Future Challenges. *Int. J. Environ. Res. Public Health* 11 (8), 8137–8165. doi:10.3390/ijerph110808137
- Chang, C., Yang, C., Liu, Y., Tao, P., Song, C., Shang, W., et al. (2016). Efficient Solar-Thermal Energy Harvest Driven by Interfacial Plasmonic Heating-Assisted Evaporation. *ACS Appl. Mater. Inter.* 8 (35), 23412–23418. doi:10.1021/acsami.6b08077
- Chen, C., Li, Y., Song, J., Yang, Z., Kuang, Y., Hitz, E., et al. (2017). Highly Flexible and Efficient Solar Steam Generation Device. *Adv. Mater.* 29 (30), 1701756. doi:10.1002/adma.201701756
- Chen, L., Xia, M., Du, J., Luo, X., Zhang, L., and Li, A. (2020). Superhydrophilic and Oleophobic Porous Architectures Based on Basalt Fibers as Oil-Repellent Photothermal Materials for Solar Steam Generation. *ChemSuschem* 13 (3), 493–500. doi:10.1002/cssc.201902775
- Chen, Y., Zhao, G., Ren, L., Yang, H., Xiao, X., and Xu, W. (2020). Blackbody-Inspired Array Structural Polypyrrole-Sunflower Disc with Extremely High Light Absorption for Efficient Photothermal Evaporation. *ACS Appl. Mater. Inter.* 12 (41), 46653–46660. doi:10.1021/acsami.0c11549
- Fang, J., Liu, J., Gu, J., Liu, Q., Zhang, W., Su, H., et al. (2018). Hierarchical Porous Carbonized Lotus Seedpods for Highly Efficient Solar Steam Generation. *Chem. Mater.* 30 (18), 6217–6221. doi:10.1021/acs.chemmater.8b01702
- Ghasemi, H., Ni, G., Marconnet, A. M., Loomis, J., Yerci, S., Miljkovic, N., et al. (2014). Solar Steam Generation by Heat Localization. *Nat. Commun.* 5 (1), 444. doi:10.1038/ncomms5449
- Jun, Y.-S., Wu, X., Ghim, D., Jiang, Q., Cao, S., and Singamaneni, S. (2019). Photothermal Membrane Water Treatment for Two Worlds. *Acc. Chem. Res.* 52 (5), 1215–1225. doi:10.1021/acs.accounts.9b00012
- Khalil, A., Amjad, M., Noor, F., Hussain, A., Nawaz, S., Filho, E. P. B., et al. (2020). Performance Analysis of Direct Absorption-Based Parabolic Trough Solar Collector Using Hybrid Nanofluids. *J. Braz. Soc. Mech. Sci. Eng.* 42 (11), 573. doi:10.1007/s40430-020-02654-2
- Kuravi, S., Trahan, J., Goswami, D. Y., Rahman, M. M., and Stefanakos, E. K. (2013). Thermal Energy Storage Technologies and Systems for Concentrating Solar Power Plants. *Prog. Energ. Combustion Sci.* 39 (4), 285–319. doi:10.1016/j.peccs.2013.02.001
- Li, X., Xu, W., Tang, M., Zhou, L., Zhu, B., Zhu, S., et al. (2016). Graphene Oxide-Based Efficient and Scalable Solar Desalination under One Sun with a Confined 2D Water Path. *Proc. Natl. Acad. Sci. U.S.A.* 113 (49), 13953–13958. doi:10.1073/pnas.1613031113
- Li, Y., Gao, T., Yang, Z., Chen, C., Kuang, Y., Song, J., et al. (2017). Graphene Oxide-Based Evaporator with One-Dimensional Water Transport Enabling High-Efficiency Solar Desalination. *Nano Energy* 41, 201–209. doi:10.1016/j.nanoen.2017.09.034
- Liu, K.-K., Jiang, Q., Tadepalli, S., Raliya, R., Biswas, P., Naik, R. R., et al. (2017). Wood-Graphene Oxide Composite for Highly Efficient Solar Steam Generation and Desalination. *ACS Appl. Mater. Inter.* 9 (8), 7675–7681. doi:10.1021/acsami.7b01307
- Liu, Y., Ai, K., Liu, J., Deng, M., He, Y., and Lu, L. (2013). Dopamine-Melanin Colloidal Nanospheres: An Efficient Near-Infrared Photothermal Therapeutic Agent for *In Vivo* Cancer Therapy. *Adv. Mater.* 25 (9), 1353–1359. doi:10.1002/adma.201204683
- Liu, Y., Chen, J., Guo, D., Cao, M., and Jiang, L. (2015). Floatable, Self-Cleaning, and Carbon-Black-Based Superhydrophobic Gauze for the Solar Evaporation Enhancement at the Air-Water Interface. *ACS Appl. Mater. Inter.* 7 (24), 13645–13652. doi:10.1021/acsami.5b03435
- Nathan, G. J., Jafarian, M., Dally, B. B., Saw, W. L., Ashman, P. J., Hu, E., et al. (2018). Solar thermal Hybrids for Combustion Power Plant: A Growing Opportunity. *Prog. Energ. Combustion Sci.* 64, 4–28. doi:10.1016/j.peccs.2017.08.002
- Ortiz, J. M., Sotoca, J. A., Exposito, E., Gallud, F., García-García, V., Montiel, V., et al. (2005). Brackish Water Desalination by Electrodialysis: Batch Recirculation Operation Modeling[J]. *J. Membr. Sci.* 252 (1-2), 65–75. doi:10.1016/j.memsci.2004.11.021
- Song, C., Li, T., Guo, W., Gao, Y., Yang, C., Zhang, Q., et al. (2018). Hydrophobic Cu<sub>12</sub>Sb<sub>4</sub>S<sub>13</sub>-Deposited Photothermal Film for Interfacial Water Evaporation and thermal Antibacterial Activity. *New J. Chem.* 42 (5), 3175–3179. doi:10.1039/c7nj04545j
- Wang, Z., Liu, Y., Tao, P., Shen, Q., Yi, N., Zhang, F., et al. (2014). Bio-Inspired Evaporation through Plasmonic Film of Nanoparticles at the Air-Water Interface. *Small* 10 (16), 3234–3239. doi:10.1002/smll.201401071
- Wang, Z., Wang, Y., Xu, G., and Ren, J. (2019). Sustainable Desalination Process Selection: Decision Support Framework under Hybrid Information. *Desalination* 465, 44–57. doi:10.1016/j.desal.2019.04.022
- Wang, Z., Yan, Y., Shen, X., Jin, C., Sun, Q., and Li, H. (2019). A Wood-Polypyrrole Composite as a Photothermal Conversion Device for Solar Evaporation Enhancement. *J. Mater. Chem. A* 7 (36), 20706–20712. doi:10.1039/c9ta04914b
- Wilson, H. M., Ahirrao, D. J., Raheman Ar, S., and Jha, N. (2020). Biomass-Derived Porous Carbon for Excellent Low Intensity Solar Steam Generation and Seawater Desalination. *Solar Energ. Mater. Solar Cell* 215, 110604. doi:10.1016/j.solmat.2020.110604
- Wu, X., Chen, G. Y., Owens, G., Chu, D., and Xu, H. (2019). Photothermal Materials: A Key Platform Enabling Highly Efficient Water Evaporation Driven by Solar Energy. *Mater. Today Energ.* 12, 277–296. doi:10.1016/j.mtener.2019.02.001
- Wu, X., Gao, T., Han, C., Xu, J., Owens, G., and Xu, H. (2019). A Photothermal Reservoir for Highly Efficient Solar Steam Generation without Bulk Water. *Sci. Bull.* 64 (21), 1625–1633. doi:10.1016/j.scib.2019.08.022
- Wu, X., Robson, M. E., Phelps, J. L., Tan, J. S., Shao, B., Owens, G., et al. (2019). A Flexible Photothermal Cotton-CuS Nanocage-Agarose Aerogel towards Portable Solar Steam Generation. *Nano Energy* 56, 708–715. doi:10.1016/j.nanoen.2018.12.008
- Xu, Y., Yang, Y., Sun, M., Fan, X., Song, C., Tao, P., et al. (2021). High-performance Desalination of High-Salinity Reverse Osmosis Brine by Direct Contact Membrane Distillation Using Superhydrophobic Membranes[J]. *J. Appl. Polym. Sci.* 138 (5), e49768. doi:10.1002/app.49768
- Xu, Y., Mu, H., Han, X., Sun, T., Fan, X., Lv, B., et al. (2021). A Simple, Flexible, and Porous Polypyrrole-wax Gourd Evaporator with Excellent Light Absorption for Efficient Solar Steam Generation. *Int. J. Energ. Res.* 45 (15), 21476–21486. doi:10.1002/er.7195
- Xu, Y., Yang, Y., Fan, X., Liu, Z., Song, Y., Wang, Y., et al. (2021). In-situ Silica Nanoparticle Assembly Technique to Develop an Omniphobic Membrane for Durable Membrane Distillation. *Desalination* 499, 114832. doi:10.1016/j.desal.2020.114832
- Xu, Y., Yuan, Y., Fan, X., Cui, M., Xiao, J., Du, J., et al. (2020). Silver Nanowire-Carbon Nanotube/Coal-Based Carbon Composite Membrane with Fascinating Antimicrobial Ability and Antibiofouling under Electrochemical Assistance. *J. Water Process Eng.* 38, 101617. doi:10.1016/j.jwpe.2020.101617
- Xue, Y., Ge, Z., Yang, L., and Du, X. (2019). Peak Shaving Performance of Coal-Fired Power Generating Unit Integrated with Multi-Effect Distillation Seawater Desalination. *Appl. Energ.* 250, 175–184. doi:10.1016/j.apenergy.2019.04.190
- Yang, J., Pang, Y., Huang, W., Shaw, S. K., Schiffbauer, J., Pillers, M. A., et al. (2017). Functionalized Graphene Enables Highly Efficient Solar Thermal Steam Generation. *ACS Nano* 11 (6), 5510–5518. doi:10.1021/acs.nano.7b00367

**Conflict of Interest:** The authors declare that the research was conducted in the absence of any commercial or financial relationships that could be construed as a potential conflict of interest.

**Publisher's Note:** All claims expressed in this article are solely those of the authors and do not necessarily represent those of their affiliated organizations or those of the publisher, the editors, and the reviewers. Any product that may be evaluated in this article or claim that may be made by its manufacturer is not guaranteed or endorsed by the publisher.

Copyright © 2022 Chen, Chen, Zang, Sha, Xiao, Wang, Wang and Wu. This is an open-access article distributed under the terms of the Creative Commons Attribution License (CC BY). The use, distribution or reproduction in other forums is permitted, provided the original author(s) and the copyright owner(s) are credited and that the original publication in this journal is cited, in accordance with accepted academic practice. No use, distribution or reproduction is permitted which does not comply with these terms.